Received: 18 November 2024 | Accepted: 17 May 2025

DOI: 10.1097/HEP.0000000000001425

ORIGINAL ARTICLE

OPEN

Refinement of histologic subtypes and identification of biomarkers linked to unfavorable prognosis in cholangiocarcinoma: The ENSCCA registries' framework for digital twin advancement

Guido Carpino[1] | Diletta Overi[1] | Rocio I.R. Macias[2] | Vincenzo Cardinale[3] | Laura Izquierdo-Sanchez[4,5] | Pilar Acedo[6] | Marco Rengo[7,8] | Michail Doukas[9] | Timothy J. Kendall[10] | Julien Calderaro[11] | Lara R. Heij[9,12,13,14] | Konrad Reichel[14] | Stefano Leone[1] | Paolo Onori[1] | Barbara Franceschini[15] | Cristiana Soldani[15] | Luca Di Tommaso[16,17] | Pedro M. Rodrigues[4,5,18] | Jérémy Augustin[11] | Raffaele Brustia[19,20,21] | Guido Torzilli[16,22] | Manuela Martin-Izquierdo[23] | Jose M. Hernández-Bayo[23] | Diego Bueno-Sacristan[24] | Ezio Lanza[25] | Andres Garcia-Sampedro[6,26] | Alberto Quaglia[27] | Francesco Ardito[28] | Agostino Maria De Rose[28] | Felice Giuliante[28] | Elio Damato[29] | Valeria Panebianco[29] | Bas Groot Koerkamp[30] | Stephen P. Pereira[6] | Gian Luca Grazi[31] | Domenico Alvaro[3] | Ana Lleo[16,32] | Jesus M. Banales[4,5,18,33] | Eugenio Gaudio[1]

[1]Department of Anatomical, Histological, Forensic Medicine and Orthopaedic Sciences, Sapienza University of Rome, Rome, Italy

[2]Laboratory of Experimental Hepatology and Drug Targeting (HEVEPHARM), National Institute for the Study of Liver and Gastrointestinal Diseases (CIBERehd), IBSAL, University of Salamanca, Salamanca, Spain

[3]Department of Translational and Precision Medicine, Sapienza University of Rome, Rome, Italy

[4]Department of Liver and Gastrointestinal Diseases, Biogipuzkoa Health Research Institute, Donostia University Hospital, University of the Basque Country (UPV/EHU), San Sebastian, Spain

[5]National Institute for the Study of Liver and Gastrointestinal Diseases (CIBERehd), Carlos III National Health Institute, Madrid, Spain

[6]Institute for Liver and Digestive Health, University College London, London, UK

[7]Department of Medical-Surgical Sciences and Biotechnologies, Sapienza University of Rome, Latina, Italy

[8]Academic Diagnostic Imaging Division, I.C.O.T. Hospital, Latina, Italy

[9]Department of Pathology and Clinical Bioinformatics, Erasmus University Medical Centre, Rotterdam, The Netherlands

[10]University of Edinburgh Centre for Inflammation Research, Institute for Regeneration and Repair, University of Edinburgh, Edinburgh, UK

[11]Department of Pathology, Assistance Publique Hôpitaux de Paris, Groupe Hospitalier Henri Mondor, Créteil, France

[12]Department of Pathology, University Hospital Essen, Essen, Germany

[13]Department of Renal and Hypertensive Disorders, Rheumatological and Immunological Diseases (Medical Clinic II), Medical Faculty, RWTH Aachen University, Aachen, Germany

[14]Department of Surgery and Transplantation, University Hospital Essen, Essen, Germany

[15]Laboratory of Hepatobiliary Immunopathology, IRCCS Humanitas Research Hospital, Rozzano, Milan, Italy

[16]Department of Biomedical Sciences, Humanitas University, Milan, Italy

[17]Pathology Unit, IRCCS Humanitas Research Hospital, Rozzano, Milan, Italy

[18]Ikerbasque, Basque Foundation for Science, Bilbao, Spain

[19]Department of Digestive and Hepato-pancreatic-biliary Surgery, Université Paris-Est Créteil, UPEC, Créteil, France

[20]Department of Digestive and Hepato-pancreatic-biliary Surgery, INSERM, Team "Virus Hépatologie Cancer," Créteil, France

[21]Department of Digestive and Hepato-pancreatic-biliary Surgery, Assistance Publique-Hôpitaux de Paris, Henri Mondor-University Hospital, Créteil, France

[22]Department of Surgery, Division of Hepatobiliary and General Surgery, IRCCS Humanitas Research Hospital, Rozzano, Milan, Italy

[23]Servicio de Radiodiagnostico, Hospital Universitario de Salamanca, IBSAL, Salamanca, Spain

[24]Servicio de Patologia, Hospital Universitario de Salamanca, IBSAL, Salamanca, Spain

[25]Division of Interventional Radiology, IRCCS Humanitas Research Hospital, Milan, Italy

[26]Department of Chemical Engineering and Biotechnology, University of Cambridge, Cambridge, UK

[27]Department of Cellular Pathology, UCL Cancer Institute, Royal Free Hospital, London, UK

[28]Hepatobiliary Surgery Unit, Foundation and Teaching Hospital Sacred Heart IRCCS A. Gemelli, Catholic University of the Sacred Heart, Rome, Italy

[29]Department of Radiological Sciences, Oncology and Pathology, Sapienza University of Rome, Rome, Italy

[30]Department of Surgery, Erasmus MC Cancer Institute, Rotterdam, The Netherlands

[31]Department of Experimental and Clinical Medicine, HepatoBiliaryPancreatic Surgery, University of Florence, Florence, Italy

[32]Department of Gastroenterology, Division of Internal Medicine and Hepatology, IRCCS Humanitas Research Hospital, Rozzano, Milan, Italy

[33]Department of Biochemistry and Genetics, School of Sciences, University of Navarra, Pamplona, Spain

Correspondence
Guido Carpino, Department of Anatomical, Histological, Forensic Medicine and Orthopaedic Sciences, Sapienza University of Rome, Via Alfonso Borelli 50, 00161 Rome, Italy.
Email: guido.carpino@uniroma1.it

Abstract

Background and Aims: Cholangiocarcinoma (CCA) displays remarkable anatomical and histological heterogeneity. Besides diagnosis confirmation, histology currently does not have a major role in the management of CCA. We aimed to study the clinical relevance of histological heterogeneity of CCA and putative tissue biomarkers by creating a multicentric digitalized European CCA Histology Registry.

Approach and Results: Nine referral centers, participating in the International Cholangiocarcinoma Clinical Registry, shared samples and data from 293 patients. Histological and immunohistochemistry stains (n = 10) were performed. Computed tomography (CT) scans (n = 112 cases) were analyzed by morphological and radiomics techniques. A selection of cases (n = 18) was processed for spatial transcriptomics analysis. No significant differences in 5-year overall survival (OS) were found in perihilar CCA versus intrahepatic (i) CCA, and in small bile duct (SBD) versus large bile duct (LBD) iCCA. When cases were classified by Periodic acid of Schiff (PAS) positivity (mucin content), PAS^{HIGH} LBD iCCA showed a significantly worse 5-year OS compared to PAS^{LOW} iCCA. Multivariate Cox regression identified PAS^{HIGH} LBD iCCA phenotype as an independent predictor of worse OS. PAS^{HIGH} LBD iCCA subtype showed specific molecular characteristics at spatial transcriptomics and immunohistochemistry; CT scans and serology could distinguish PAS^{HIGH} LBD iCCA phenotype with excellent accuracy.

Abbreviations: CCA, cholangiocarcinoma; cHCC-CCA, combined hepatocellular carcinoma–cholangiocarcinoma; dCCA, distal cholangiocarcinoma; DSP, digital spatial profiler; ENSCCA, European Network for the Study of Cholangiocarcinoma; EpCAM, Epithelial Cell Adhesion Moelcule; FFPE, formalin-fixed paraffin-embedded; H&E, hematoxylin and eosin; iCCA, intrahepatic cholangiocarcinoma; INT-CCA, International Cholangiocarcinoma; LBD, large bile duct; MVD, microvascular density; OS, overall survival; PAS, Periodic acid of Schiff; pCCA, perhilar cholangiocarcinoma; PCNA, Proliferating Cell Nuclear Antigen; PNI, perineural invasion; SBD, small bile duct; vWF, von Willebrand Factor; WSI, whole slide imaging.

Carpino Guido and Overi Diletta are co-first authors.

Supplemental Digital Content is available for this article. Direct URL citations are provided in the HTML and PDF versions of this article on the journal's website, www.hepjournal.com.

Conclusions: Our data underline the importance of identifying morphological subclasses with a significant prevalence in CCA as a tool for risk stratification and prognosis. The European CCA Histology Registry represents a valuable platform for integrating digital pathology with clinical, radiological, and molecular information as a framework for digital twin advancement.

Keywords: biliary tract cancer, cell of origin, digital pathology, primary liver cancer, spatial transcriptomics

INTRODUCTION

Cholangiocarcinoma (CCA) is a malignant tumor arising in the biliary tree.[1,2] The incidence of CCA currently accounts for ~15% of primary hepatobiliary cancers, and its mortality represents ~2% of all cancer-related deaths worldwide.[3]

CCA is classified into 3 anatomical subtypes: intrahepatic (iCCA), perihilar (pCCA), and distal (dCCA);[4] each anatomical subtype should be considered as an independent entity from a biological and clinical point of view.[5] CCA also displays remarkable histological heterogeneity, with the small and large bile duct (SBD and LBD, respectively) types being the most common morphologies in iCCA.[4] The histological appearance has been ascribed to the duct of origin and is associated with type-specific molecular signatures.[6]

Histologic tumor characterization is well-established in other malignancies as the basis for risk stratification and targeted therapy; for example, lung cancers are managed differently based on the cell morphology at histologic evaluation,[7] and immunohistochemistry defines therapeutic options and clinical management in those affected by breast cancer.[8] Recent clinical practice guidelines have suggested classifying iCCA according to the morphological type based on histological assessment[5] although the strength of evidence for the value of histological classification is limited by conflicting published data,[9–12] the lack of multicenter studies, and small sample sizes.[5] Therefore, aside from confirming the diagnosis, histological classification does not yet contribute to the management of people affected by CCA.[2,5] However, the morphology of tumors could reflect their genetic background and behavior,[13,14] and critically evaluating the histological characteristics of CCA may reveal key information for risk stratification and therapy choice. Personalized therapy may, therefore, require careful integration of individual morphological features and biomarkers, representing a "next-generation pathology" approach.[15]

To address this challenge, we created a European multicentric web-based platform for digital histological images using whole-slide imaging technology. This registry was built upon a patient cohort with comprehensive clinical records[16] and access to various biological samples (eg, paraffin-embedded and/or frozen tissues, serum, bile), along with radiological images including CT scans. The present study analyses a cohort of patients with CCA from this registry employing a multilayer approach, placing particular emphasis on specific histological features and their clinical relevance. Furthermore, we explored the potential of the European CCA Histology Registry as a multimodal platform for integrating digital pathology with clinical, radiological, and molecular information.

METHODS

Study design and data collection

The European CCA Histology Registry, endorsed by the European Network for the Study of Cholangiocarcinoma (ENSCCA), represents a digitalized repository of stained slides obtained from individuals who underwent liver resection with curative intent for CCA. Recruitment to the registry was facilitated through the collaboration of 9 referral healthcare centers across 6 European countries (Italy, the Netherlands, Spain, the United Kingdom, France, and Germany). Individuals diagnosed with CCA within a 12-year period (January 1st, 2010, to December 31st, 2021) were considered for inclusion in the registry study. Eligibility criteria included: (i) availability of a formalin-fixed paraffin-embedded (FFPE) block containing tumor from the resection specimen; (ii) accessibility of snap frozen samples; (iii) comprehensive clinical information documented in the International Cholangiocarcinoma (INT-CCA) Registry; and (iv) availability of stored serum sample. Accordingly, individuals meeting all inclusion criteria were identified, and FFPE 3 μm-thick sections of resected CCA samples (N = 15) were collected from the Pathology Department of each participating institution. These samples were sent to Sapienza University of Rome for inclusion in the registry. Whenever possible, non-tumoral surrounding liver was present in the provided sections.

Individual patient data that had been obtained from medical records by the participating hospitals and

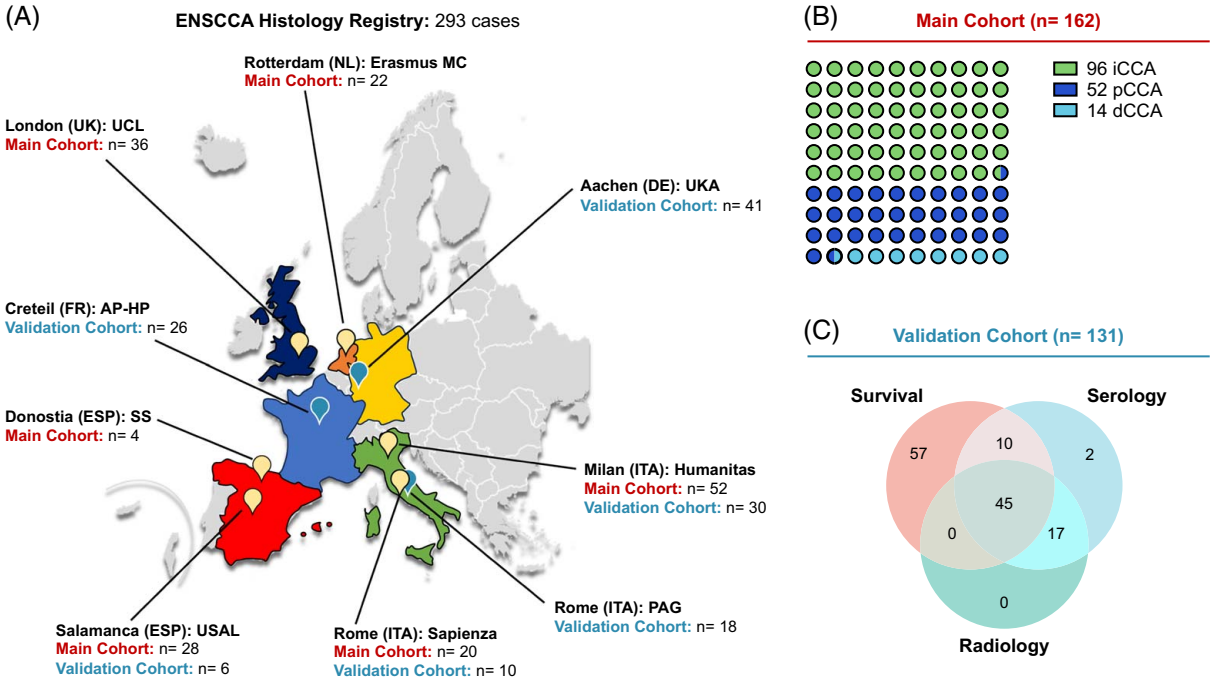

FIGURE 1 Geographical distribution and anatomical subtypes of cholangiocarcinoma (CCA) cases in the European CCA Histology Registry. (A) Geographical distribution of contributing centers and number of cases included in the European CCA Histology Registry. (B) Main cohort: the waffle chart represents the percentage of each anatomical subtype observed in the main cohort. (C) Validation cohort: the Venn diagram summarizes the number of cases extracted from the validation cohort and used for each validation analysis. Abbreviations: dCCA, distal CCA; iCCA, intrahepatic CCA; pCCA, perihilar CCA.

included in the INT-CCA registry were retrieved, as described elsewhere.[16] Anatomical classification (iCCA, pCCA, or dCCA) followed the ICD-11 criteria.[5,17] TNM stage was extracted from investigator-reported notes in the INT-CCA registry and was derived by either histology or imaging techniques, according to the AJCC/UICC staging system, 8th edition.

All research was conducted in accordance with both the Declarations of Helsinki and Istanbul. The ENSCCA Registry Study protocol was approved by the Ethics Committee of Sapienza University of Rome, Rome, Italy (Code: 4492), serving as the coordinating center. Additionally, each participating center secured local ethical approval (or equivalent) and finalized a Material Transfer Agreement with the Sapienza University of Rome. Written informed consent was given by all subjects. Samples and clinical data were pseudonymized.

Histology and immunohistochemistry

FFPE sections were processed for routine histological stains, including hematoxylin and eosin (H&E), Periodic acid of Schiff (PAS), and Sirius Red/Fast Green. Moreover, a custom immunohistochemical panel was designed covering epithelial and stromal markers. The list of targets and primary antibodies is provided in Supplemental Table S1, http://links.lww.com/HEP/J843. Immunohistochemistry was performed by using standard procedures (see Supplemental Digital Content for further details, http://links.lww.com/HEP/J844).

All stained slides were scanned by a digital scanner (Aperio Scanscope CS System, Aperio Digital Pathology, Leica Biosystems) and processed by ImageScope. The digital registry was populated by creating a pseudonymized folder for each patient using the eSlideManager software (Aperio Scanscope CS System, Aperio Digital Pathology, Leica Biosystems).

LBD type was defined from H&E-stained sections as a tumor composed of columnar cells forming large infiltrating glandular structures; similarly, SBD type was defined as tumors composed of cuboidal cells arranged as small to intermediate-sized tubules or anastomosing glands. Cholangiolo-cellular subtype was considered to be a subtype of SBD. Rare variants and combined hepatocellular carcinoma–cholangiocarcinoma (cHCC-CCA) were diagnosed based on criteria described in the World Health Organization "blue book."[18]

Mucin content was quantified on PAS-stained sections. Mucin was assessed in tumoral glands based on the presence of intraluminal PAS positivity and/or intracellular PAS-positive vacuoles in the apical cytoplasm.[19] The percentage of glandular structures positive for PAS was counted, and then a semi-quantitative scoring system was applied (0: $\leq$1%; 1: 1%–10%; 2: 11%–30%; 3: 31%–50%; 4: $>$50%). Tumors were defined as PAS^{HIGH} (PAS positivity score $>$1) or PAS^{LOW}. For Epithelial Cell Adhesion

Molecule (EpCAM) and Proliferating Cell Nuclear Antigen (PCNA) stains, the percentage of positive cells was counted, and then a semi-quantitative scoring system was applied (0: ≤1%; 1: 1%–10%; 2: 11%–30%; 3: 31%–50%; 4: >50%). Microvascular density (MVD) was assessed on von Willebrand Factor (vWF) stain as the number of microvessels within each 40× magnification high-powered field.[19] All morphological and immunohistochemical features were independently assessed by 2 researchers in a blinded manner. In case of disagreement, a joint review of the slides was performed and a consensus reached.

N = 162 patients coming from 6 centers who received treatment between 2016 and 2023 were processed for all stains and represent the main exploratory cohort for this study. N = 131 cases with histology were included during 2024 and 2025; these cases were used as a validation cohort (Survival, Serology, Radiology) based on the availability of survival data (n = 112), serology (n = 74), and CT scan (n = 62), respectively (Figure 1).

Spatial molecular profiling

FFPE sections of 18 iCCA were selected for 2 separate analyses (#1: 6 SBD and 6 PAS^{HIGH} LBD types; #2: 3 PAS^{LOW} LBD and 3 PAS^{HIGH} LBD types) on the NanoString GeoMx Digital Spatial Profiler (DSP). Slides were prepared according to the manufacturer's protocol. The slides were processed by using the GeoMx Solid Tumor TME Morphology Kit (code #121300310, including fluorescent antibodies against Pan-Cytokeratin, CD45, and the nuclear stain SYTO13) and the GeoMx Immune Pathways Panel (code #121300201, RNA assay including 84 targets plus controls for human).

The whole slides were imaged using the GeoMx DSP and the integrated software suite used to select regions of interest within the tumor mass. Pan-Cytokeratin and CD45 were used for the segmentation of epithelial and immune cell fractions, from which DNA oligo probes were photocleaved and cell-type-specific transcriptomic profiles obtained. The readout of collected probes was performed according to the manufacturer's protocol by using the nCounter Sprint. Reporter Code Count (RCC) files were uploaded into the GeoMx DSP for mapping data to the spatial origin; data were processed by GeoMX DSP Analysis Suite (v 3.0.0113) for quality control, normalization and background correction, and expression analysis.

Radiology and radiomics

CT datasets were acquired on different multidetector scanners ranging from 16 to 128 rows. A 120 kV tube voltage was used for all acquisitions. Only portal venous phases were analyzed. The portal venous phase was acquired after 75 seconds from the injection of iodinated contrast (0.625 mL/kg of total body weight at a rate of 1.6 gl/s).

All CT datasets were anonymized and collected on a free and open-source code software program (Horosproject.org, Nimble Co LLC d/b/a Purview). Images acquired from the diaphragmatic dome to the lower margin of the liver were selected for further analysis, and the selected volume was transferred to a dedicated platform for tumor segmentation and radiomic feature extraction (3D Slicer, http://www.slicer.org). Tumor segmentation was performed by an expert radiologist. All axial images of the tumor were contoured, resulting in a 3D region of interest.

For each tumor, 13 morphologic features were evaluated by 2 independent radiologists. For each 3D region of interest, corresponding to the entire volume of the selected liver lesion, 74 features were extracted using Radiomics, an extension for 3D Slicer that encapsulates the pyradiomics library. Morphologic and radiomic features are reported in Supplemental Digital Content, http://links.lww.com/HEP/J844.

CT features were analyzed using the WEKA (Waikato Environment for Knowledge Analysis, Version 3.8.5, University of Waikato) machine learning suite for data mining classification.

Radiological features were assessed alongside histological classifications of morphological tumor features. Two classifications were performed: SBD versus LBD, and PAS^{HIGH} LBD versus other histotypes. For each classification, 3 models were built: (i) Morphology model; (ii) Radiomic model; (iii) Combined model.

The main radiological cohort was first divided into 2 groups using the WEKA Explorer Filter tool; two-thirds of the patients were randomized to the training group and one-third to the validation group. The training group was analyzed using Auto-WEKA. The optimized models were applied to the corresponding validation groups. For each classification model, sensitivity, specificity, accuracy, and AUC were evaluated.

Statistical analysis

Baseline demographics and risk factors were summarized using descriptive statistics. Continuous data were described as median (IQR), while categorical variables were summarized as n (%). The Student *t* test or the Mann–Whitney *U* test was used to determine differences between groups for normally or non-normally distributed data, respectively. The Fisher exact test was used to compare categorical variables between the subgroups. OS was assessed as the time from diagnosis to death or last medical visit. Relapse-free survival was calculated as the time from tumor resection to the event of relapse or death. Patients with no information on survival, lost to

TABLE 1 Baseline cholangiocarcinoma (CCA) patient characteristics and tumor presentation at diagnosis

	All CCA (n = 162)	iCCA (n = 96)	pCCA (n = 52)	dCCA (n = 14)	*p*-value iCCA vs. pCCA
Gender, n (%)					
Female	63 (39)	44 (46)	15 (29)	4 (29)	ns
Age, median [IQR]	69 [61–74]	69 [62–74]	65 [54–75]	77 [71–79]	ns
BMI, median [IQR]	25 [23–28]	24 [23–28]	25 [22–27]	25 [24–27]	ns
Stage, n					
I	39	35	3	1	
II	56	27	17	12	
III	50	27	23	0	
IV	17	7	9	1	
Stage, n (%)					
I–II	95 (59)	62 (65)	20 (38)	13 (93)	
III–IV	67 (41)	34 (35)	32 (62)	1 (7)	$p =$ **0.0031**
T, n					
1	43	39	3	1	
2	65	36	25	4	
3	48	20	19	9	
4	6	1	5	0	
T, n (%)					
1–2	108 (67)	85 (89)	28 (54)	5 (36)	
3–4	54 (33)	21 (11)	24 (46)	9 (54)	$p =$ **0.0012**
N+, n (%)	40 (25)	15 (16)	21 (40)	4 (29)	$p =$ **0.0012**
M1, n (%)	12 (8)	7 (7)	5 (10)	1 (7)	ns
Tobacco, n (%)	39 (24)	29 (30)	5 (10)	5 (36)	$p =$ **0.0021**
Alcohol	20 (12)	9 (9)	6 (11)	5 (36)	ns
Viral hepatitis	6 (4)	6 (6)	0 (0)	0 (0)	ns
PSC	6 (4)	1 (1)	5 (10)	0 (0)	$p =$ **0.0265**
Cirrhosis	8 (5)	5 (5)	3 (6)	0 (0)	ns

Abbreviations: dCCA, distal CCA; iCCA, intrahepatic CCA; ns, not significant; pCCA, perihilar CCA; PSC, primary sclerosing cholangitis.

follow-up, or alive at the last medical visit were censored at the date of the latest record. Survival analysis was performed with the Kaplan–Meier method and Cox regression. The Log-rank test was used for comparisons of Kaplan–Meier curves. HR, 95% CI, and *p* values for prognostic factors were calculated.

For radiomics, the one-way ANOVA with the Fisher LSD test was used to find significant differences in radiomic features. The reproducibility of the morphologic feature evaluation was calculated with the weighted Cohen kappa analysis. Agreement was interpreted according to the following criteria: >0.81: excellent agreement; 0.61–0.80: good agreement; 0.41–0.60: moderate agreement; 0.21–0.40: fair agreement; <0.20: poor agreement.

Predictive accuracy of serological markers was evaluated using receiver operating curves. To combine serological biomarkers, a logistic regression model was estimated with ALP, GGT, and carbohydrate antigen 19-9 (CA19-9) as the explanatory variables, and then a receiver operating curve was obtained by using the predicted probability as the test variable. The optimal cutoff value was chosen to maximize the Youden index.

Statistical analyses were performed with IBM SPSS Statistics Version 25.0 (IBM Corp.) and Graphpad Prism version 9.0 (Graphpad Software). All *p* values were obtained in 2-tailed tests, and $p < 0.05$ was considered statistically significant.

RESULTS

Digital case series creation and subject characteristics

Histological samples from n = 162 subjects with resected CCA were collected and processed. A specific digital folder containing all slides is available for each subject in the slide manager system. Subjects were divided according to the tumor anatomical location (Figure 1) into iCCA (n = 96), pCCA (n = 52), and dCCA (n = 14).

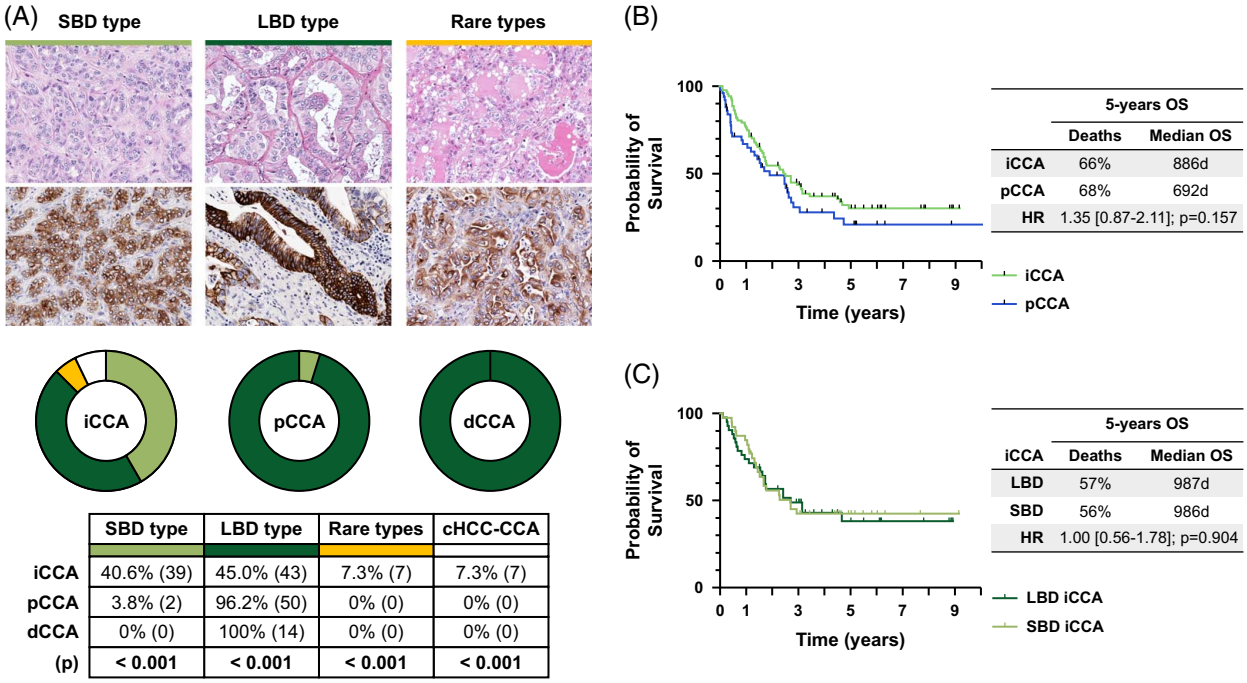

	SBD type	LBD type	Rare types	cHCC-CCA
iCCA	40.6% (39)	45.0% (43)	7.3% (7)	7.3% (7)
pCCA	3.8% (2)	96.2% (50)	0% (0)	0% (0)
dCCA	0% (0)	100% (14)	0% (0)	0% (0)
(p)	< 0.001	< 0.001	< 0.001	< 0.001

FIGURE 2 Histological subtyping of cholangiocarcinoma (CCA). (A) H&E stain (upper panels) and immunohistochemistry for CK7 (lower panels) on SBD CCA, LBD CCA, and rare CCA variants (rare types). The donut charts and the table report the distribution of histological subtypes within each anatomical type expressed as a percentage (number) of cases. Statistical significance in A was assessed by the Fisher exact test. (B, C) Kaplan–Meier curves, HR, and 95% CI for 5-year overall survival (OS) of patients based on (B) anatomical tumor subtypes (iCCA vs. pCCA) and (C) histological subtypes (SBD iCCA vs. LBD iCCA). Abbreviations: cHCC-CCA, combined hepatocellular carcinoma–CCA; CK7, cytokeratin 7; dCCA, distal CCA; H&E, hematoxylin and eosin; iCCA, intrahepatic CCA; LBD, large bile duct type; pCCA, perihilar CCA; SBD, small bile duct type.

The baseline patient characteristics and tumor presentation at diagnosis are reported in Table 1 and Supplemental Figure S1, http://links.lww.com/HEP/J845. No significant differences in gender and age at presentation were found between the different anatomical subtypes. Given the relatively low number of dCCA, statistical comparisons were not performed for this tumor subtype.

In this cohort, pCCA presented with a higher T and N compared to iCCA, thus resulting in a lower percentage of subjects with earlier disease stages (stages I and II). No difference was reported in M status (distant metastasis). Radical resection (ie, R0) was more frequently obtained in iCCA compared with pCCA (Supplemental Figure S1, http://links.lww.com/HEP/J845).

Histologic subtyping of CCA

The histologic classification was based on assessment of H&E-stained sections. Intrahepatic CCAs were classified into SBD type, LBD type, or rare variants (Figure 2A). SBD type and LBD type accounted for 40.6% and 45.0%, respectively. Remaining iCCA were classified as rare variants (7.3%) or cHCC-CCA (7.3%). Since cHCC-CCA should be considered as a separate entity,[20] these cases (n = 7) were excluded from subsequent analyses. Similarly, rare types were excluded given the low number of cases and their heterogenous phenotype (list of found rare variants is reported in Supplemental Table S2, http://links.lww.com/HEP/J843). No differences were present in terms of age, gender, stage, TNM, and residual tumor (R) between SBD and LBD types of iCCA (Supplemental Figure S1, http://links.lww.com/HEP/J845 and Supplemental Table S3, http://links.lww.com/HEP/J843).

Despite more advanced stages at diagnosis, no significant difference in 5-year OS was found in pCCA compared with iCCA (Figure 2B), nor comparing extrahepatic CCA (pCCA plus dCCA) with iCCA (Supplemental Figure S2, http://links.lww.com/HEP/J845); SBD-type and LBD-type iCCA did not differ in 5-year OS (Figure 2C). To exclude the presence of potential biases due to staging systems, we confirmed these results also after excluding stage IV and/or M1 cases from the examined cohorts (Supplemental Figure S3, http://links.lww.com/HEP/J845) and stage II iCCA with multiple nodules (Supplemental Figure S4, http://links.lww.com/HEP/J845).

The histology of p/dCCA was uniform; most cases showed histological features corresponding to conventional adenocarcinoma with large glandular elements growing within the duct wall in a periductal infiltrating

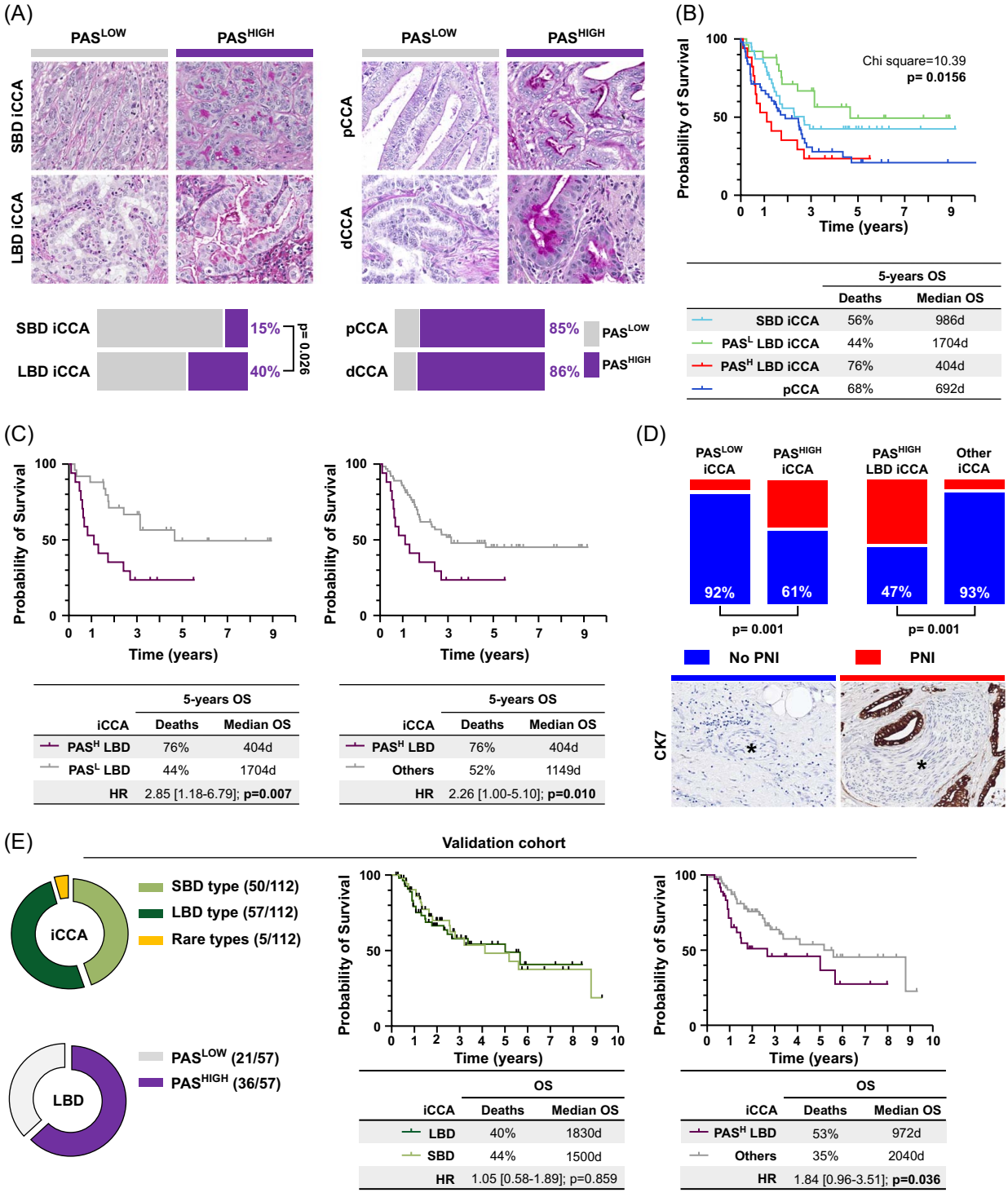

FIGURE 3 Mucin content and perineural invasion in anatomical and histological cholangiocarcinoma (CCA) subtypes. (A) PAS stain on CCA anatomical and histological subtypes. Tumors were classified as PAS^{LOW} (gray) or PAS^{HIGH} (purple). Histograms report the percentage of PAS^{LOW} and PAS^{HIGH} cases within anatomical and histological subtypes. (B) Kaplan–Meier curve for 5-year overall survival (OS) of patients based on anatomical and histological subtypes. (C) Kaplan–Meier curve, HR, and 95% CI for 5-year OS of patients based on histological iCCA subtypes. (D) Histograms report the percentages of cases displaying or not PNI in histological iCCA subtypes. Representative images from CK7 immunohistochemistry on iCCAs without (blue) or with (red) PNI. Asterisks indicate nerves. Statistical significance in A and D was assessed by the Fisher exact test. (E) Validation cohort for OS. The donut charts report the distribution within the cohort of histological subtypes (upper chart), and of PAS^{HIGH} or PAS^{LOW} cases in LBD-type iCCA (lower chart), expressed as a percentage of cases. Kaplan–Meier curve and survival analysis are reported for the OS of patients based on histological iCCA subtypes. Abbreviations: CK7, cytokeratin 7; dCCA, distal CCA; iCCA, intrahepatic CCA; LBD, large bile duct type; PAS, Periodic acid of Schiff; pCCA, perihilar CCA; PNI, perineural invasion; SBD, small bile duct type.

pattern. Unexpectedly, 2/52 pCCA showed a histology phenotype comparable to SBD iCCA subtype, as part of a mass-forming component (Supplemental Figure S5, http://links.lww.com/HEP/J845).

Histologic analysis of the surrounding non-tumoral liver

In cases where non-tumoral liver was available for assessment, a histopathological evaluation of the tissue was performed (Supplemental Figure S6, http://links.lww.com/HEP/J845). In all, 70 of 110 subjects i/pCCA cases with assessable non-tumoral liver (64%) showed evidence of chronic injury in non-lesional liver parenchyma or bile duct wall. We focused on the presence of specific patterns of hepatic (ie, fibrosis, steatosis, and lobular inflammation) and biliary (inflammation of large intrahepatic bile ducts and primary sclerosing cholangitis) injury. Hepatocyte steatosis was more frequent in non-tumoral livers from cases of iCCA (38%) compared to pCCA (6%, $p < 0.001$), while cholangitis of large intrahepatic bile ducts was more frequently present in pCCA (52%) compared to iCCA (11%, $p < 0.001$). On the other hand, no differences in the non-lesional liver were found comparing the SBD-type versus LBD-type iCCA cases. Interestingly, although the majority (45/74: 61%) of iCCA-affected subjects had significant histological liver injury, only 26% of subjects were reported to have an underlying liver disease in the available clinical records. Similarly, nearly half of the subjects with pCCA showed histologic signs of large bile duct inflammation or, when confirmed by clinical records, definite primary sclerosing cholangitis.

Mucin content and perineural invasion indicate a worse prognosis in subjects with CCA

For better identification of morphologic features with clinical relevance associated with CCA subtypes, mucin content was analyzed by a routine histologic stain (Figure 3A). Tumors were dichotomized as PAS^{HIGH} or PAS^{LOW} using a positivity cutoff of 10% (score > 1). The vast majority of p/dCCA (85% and 86%) were categorized as PAS^{HIGH}, while 23/96 (24%) iCCA were PAS^{HIGH} ($p < 0.001$ vs. p/dCCA). High PAS positivity was more frequent in LBD type (17/43: 40%) compared to SBD-type iCCA (6/39: 15%; $p = 0.023$). The second review of these PAS^{HIGH} SBD-type tumors showed that 3 of them were composed of relatively narrow tubular structures lined by cuboidal cells (3/6). The other 3 tumors, in addition to a predominant typical SBD-type appearance, also showed limited LBD-type areas in places.

In terms of outcomes, PAS^{HIGH} LBD-type iCCA showed a significantly worse 5-year OS compared to PAS^{LOW} LBD or compared to all other histologic subtypes (Figure 3B-C). Interestingly, the PAS^{HIGH} LBD-type iCCA showed similar OS to pCCA (Figure 3B and Supplemental Figure S3, http://links.lww.com/HEP/J845) and extrahepatic CCA (Supplemental Figure S2B, http://links.lww.com/HEP/J845). The results on the association between histo-typing and OS were confirmed in the validation cohort ($n = 112$, Supplemental Table S4, http://links.lww.com/HEP/J843) reported in Figure 3E.

Next, the frequency of perineural invasion (PNI) was evaluated (Figure 3D and Supplemental Figure S7, http://links.lww.com/HEP/J845). PNI was significantly more prevalent in pCCA and dCCA (70% and 54%, respectively) compared with iCCA (16%). Within iCCA, the LBD type exhibited 10-fold higher PNI frequency than other iCCA histotypes. Interestingly, PNI was more frequent in PAS^{HIGH} LBD-type iCCA compared to PAS^{LOW} iCCA (Figure 3D). Furthermore, the presence of PNI significantly correlated with worse 5-year OS (Supplemental Figure S7, http://links.lww.com/HEP/J845) and the combination of PAS^{HIGH} LBD phenotype together with PNI individuated tumors with a dismal prognosis compared to others (Supplemental Figure S7, http://links.lww.com/HEP/J845).

Spatial molecular analysis identifies iCCA subtype-specific molecular traits

Spatial molecular analysis represents a unique tool for dissecting the tumor epithelial cell from the stromal/immune cell fraction, allowing a separate analysis of each fraction (Figure 4 and Supplemental Figure S8A, http://links.lww.com/HEP/J845). The European CCA Histology Registry was used for representative case selection and subsequently to confirm the obtained preliminary results in the entire cohort. Spatial molecular analysis was performed by comparing epithelial tumor cells from the two most different histologic phenotypes, namely PAS^{HIGH} LBD ($n = 6$) versus PAS^{LOW} SBD iCCA ($n = 6$). (Figure 4 and Supplemental Figure S8B, http://links.lww.com/HEP/J845).

Among examined genes, EPCAM and HIF1A were the most upregulated and downregulated in PAS^{HIGH} LBD compared to PAS^{LOW} SBD-type iCCA, respectively (Figure 4B and Supplemental Figure S8B, http://links.lww.com/HEP/J845). Regarding markers of proliferation, PAS^{LOW} SBD-type iCCA showed upregulation in CCND1 (cyclin D1); however, no differences were present in Ki67 expression (MKI67). No differences were found in genes related to cell apoptosis. A slight but significant difference in expression was observed in some cytokines (eg, IL12B, IL6, IFNG, CCL5) (Supplemental Figure S8B, http://links.lww.com/HEP/J845).

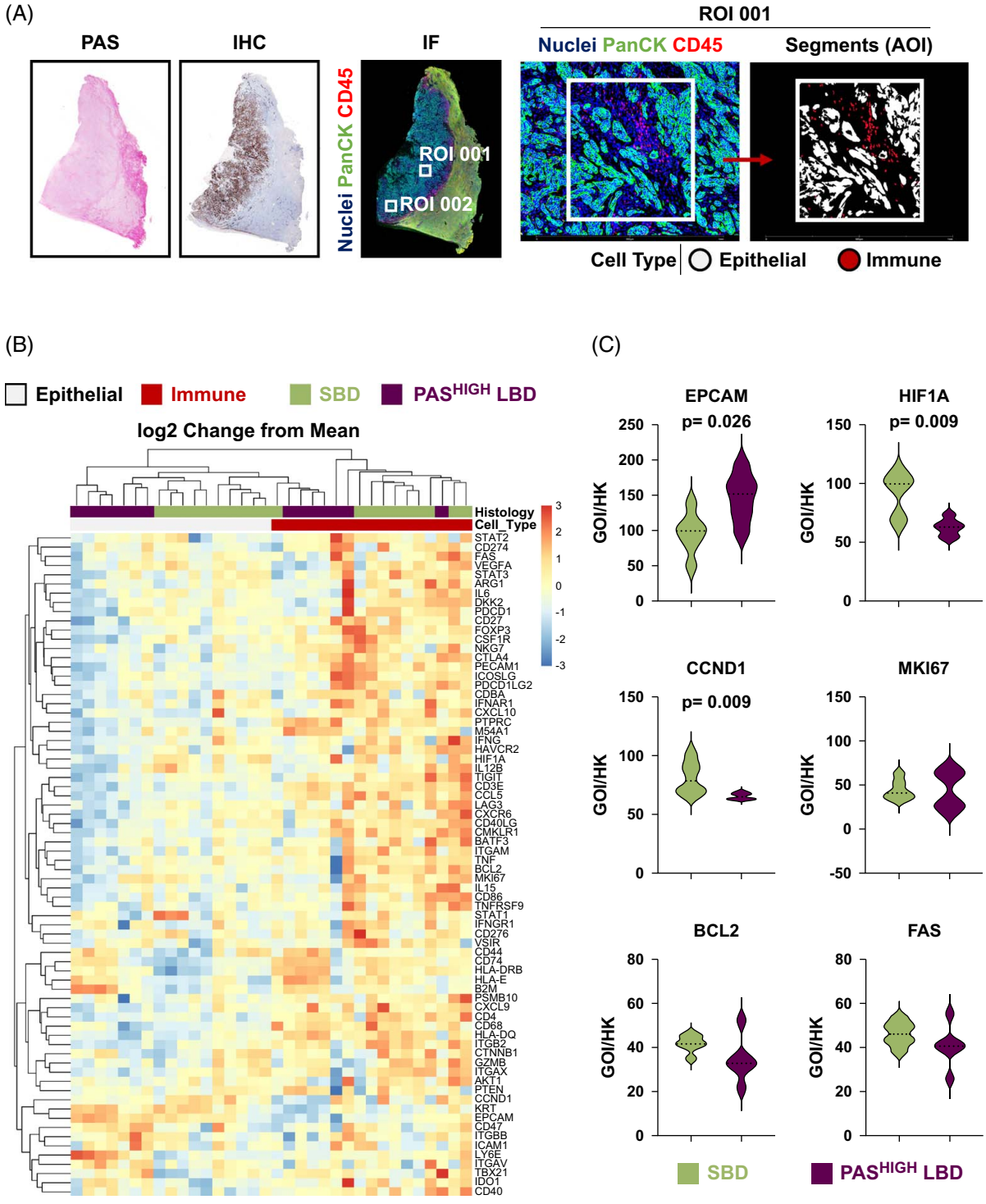

FIGURE 4 Spatial transcriptomic analysis of intrahepatic cholangiocarcinoma (iCCA) histological subtypes. (A) N = 6 SBD iCCA and N = 6 PAS^{HIGH} LBD iCCA samples from the European CCA Histology Registry were selected for spatial transcriptomic analysis. Based on immunofluorescence for PanCK and CD45, ROIs were segmented in areas of illumination (AOIs) for separate profiling of epithelial and immune cell compartments. (B) Heat map and hierarchical clustering of gene expression in iCCA show separation between epithelial and immune cells and histological subtypes. (C) Violin plots of selected genes in SBD iCCA versus PAS^{HIGH} LBD iCCA. Gene of interest (GOI) expression was normalized by housekeeping (HK) genes. Statistical significance was assessed by the Student *t* test. Abbreviations: iCCA, intrahepatic CCA; IF, immunofluorescence; IHC, immunohistochemistry; LBD, large bile duct type; PanCK, pan-cytokeratin; PAS, Periodic acid of Schiff; SBD, small bile duct type.

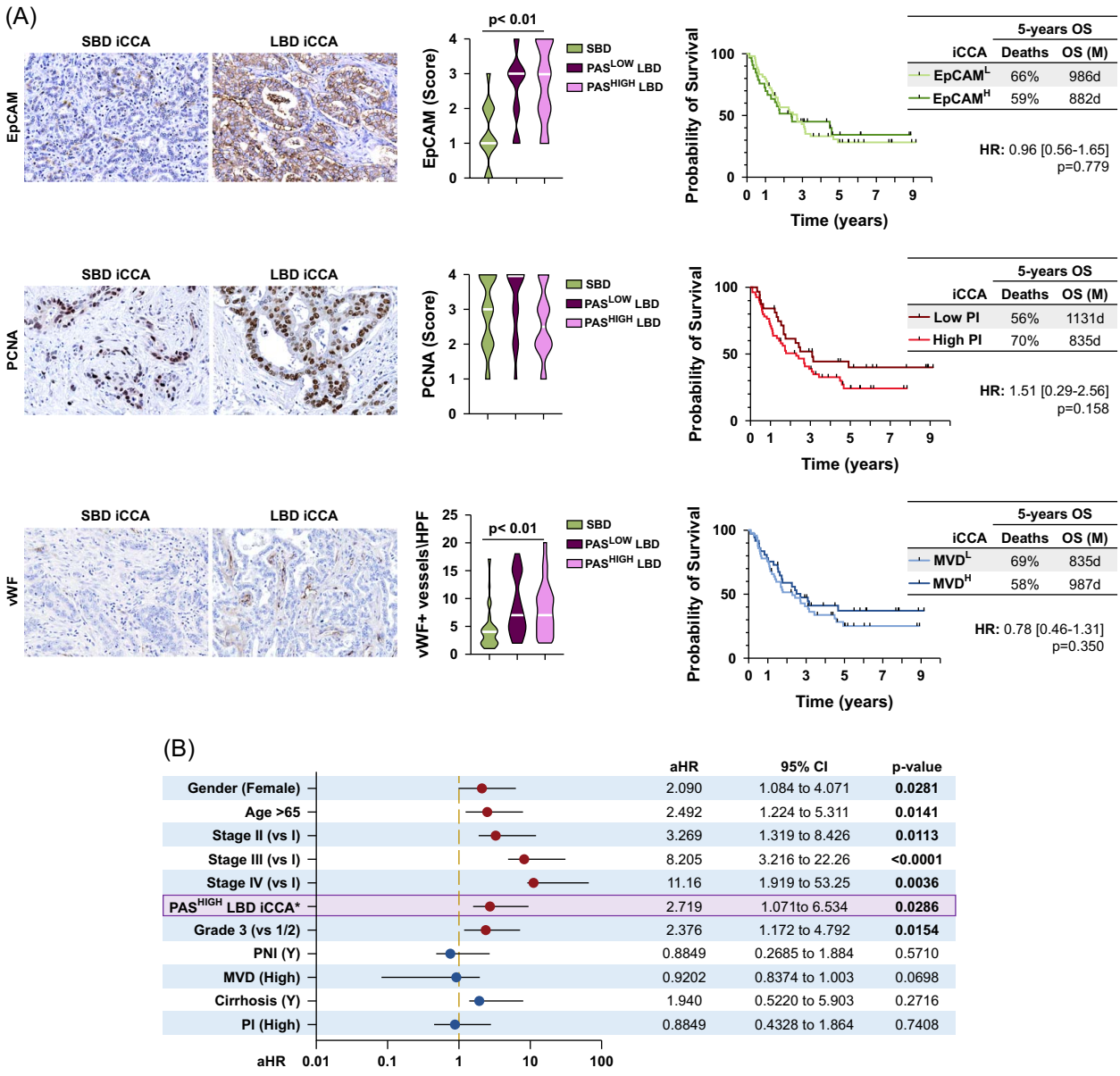

FIGURE 5 Immunohistochemical characterization of intrahepatic cholangiocarcinoma histological subtypes. (A) Immunohistochemistry for Epithelial Cell Adhesion Molecule (EpCAM), Proliferating Cell Nuclear Antigen (PCNA), and von Willebrand Factor (vWF) on SBD and LBD iCCA. Violin plots report median and interquartile range for positivity scores (EpCAM and PCNA) and for the number of vWF+ vessels per high-powered field (HPF) on SBD iCCA and PAS^{LOW}/PAS^{HIGH} LBD iCCA. Kaplan–Meier curve, HR, and 95% CI for 5-year overall survival (OS) of patients based on high versus low EpCAM positivity, proliferation index (PI), and microvascular density (MVD). (B) Forest plot illustrating independent predictors of patient survival as analyzed by multiple linear regression. *PAS^{HIGH} LBD iCCA versus other histological iCCA subtypes. Abbreviations: aHR, adjusted hazard ratio; iCCA, intrahepatic CCA; LBD, large bile duct type; SBD, small bile duct type.

In a separate experiment (Supplemental Figure S9, http://links.lww.com/HEP/J845), we performed spatial molecular analysis comparing PAS^{HIGH} versus PAS^{LOW} LBD iCCAs; no significant differences were observed in the expressions of genes identified in the PAS^{HIGH} LBD versus PAS^{LOW} LBD comparison, suggesting a close relationship among LBD subtypes.

To support these observations, we analyzed the digital slides included in the European CCA Histology Registry (ie, immunohistochemistry for EpCAM, PCNA, and vWF) in order to corroborate or validate the molecular analyses and to explore correlations with patient prognosis in the entire iCCA cohort (Figure 5A).

For EpCAM, PAS^{HIGH} LBD-type iCCA showed higher positivity compared to the SBD type. Moreover, in accordance with HIF1A gene expression, there was a lower MVD in SBD compared to PAS^{HIGH} LBD iCCA, as assessed on vWF stains. Finally, no significant differences in proliferation between iCCA subtypes were present by evaluating the immunohistochemical positivity of PCNA, a pan-cycle marker of cell proliferation. The analysis of OS

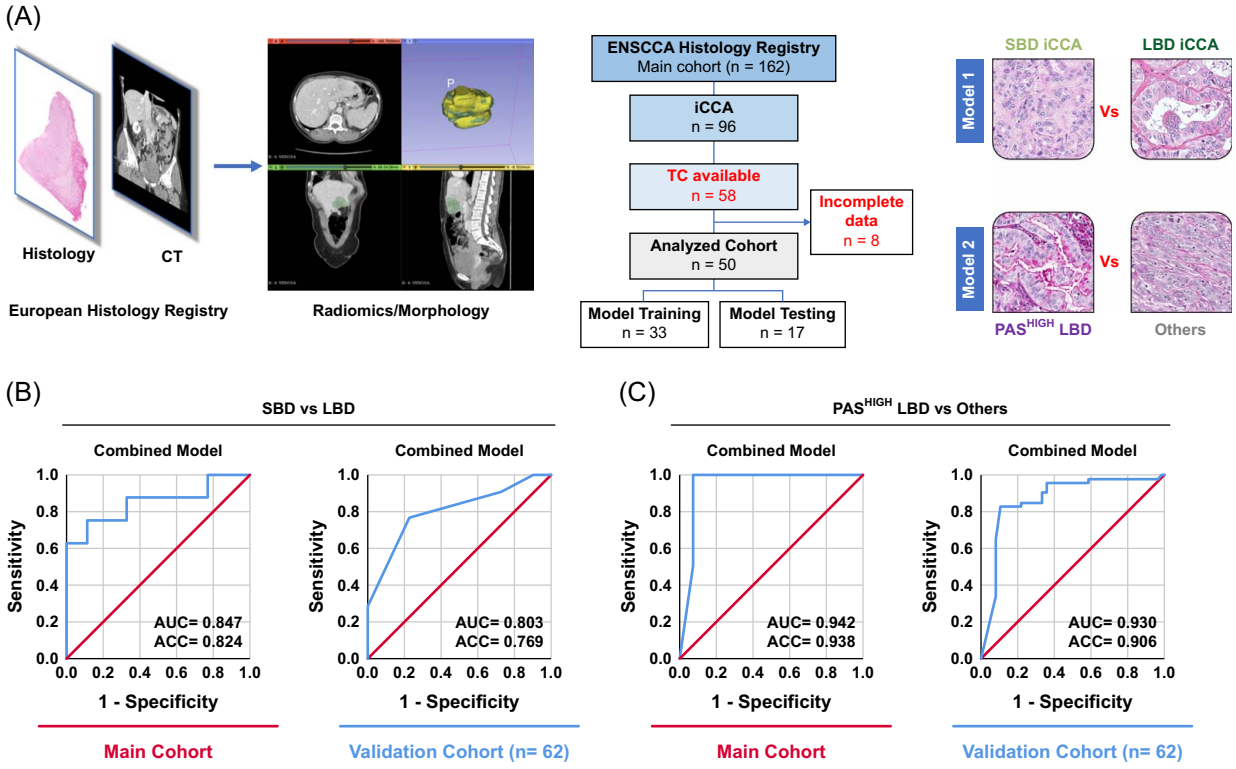

FIGURE 6 Radiological features and radiomics predictors of intrahepatic cholangiocarcinoma (iCCA) histological subtypes. (A) We analyzed morphological and radiomics CT features from patients in the histological registry for whom matched radiological images were available. A flowchart describes case selection. Two classifications of iCCA were performed: SBD versus LBD iCCA and PAS^{HIGH} LBD versus other iCCA histotypes. (B, C) ROC curves report the accuracy of the combined (radiomics + morphology) model in discriminating SBD versus LBD iCCA (B) and PAS^{HIGH} LBD versus other iCCA histotypes (C) in the main and validation cohorts. Abbreviations: ACC, accuracy; iCCA, intrahepatic CCA; LBD, large bile duct type; ROC, receiver operating curve; SBD, small bile duct type.

showed that EpCAM positivity, MVD, and proliferation index were not associated with the prognosis at 5 years.

Multivariate analyses of tissue biomarkers

To test the prognostic role of histological subtyping and other assessed histologic features (PNI, MVD, Proliferation Index), multivariate Cox regression analyses were performed by also including covariates with a potential influence on prognosis: age (> 65 years), gender, stage, tumor grade, and histologic evidence of cirrhosis. Interestingly, the PAS^{HIGH} LBD-type iCCA phenotype (Figure 5B) or high PAS positivity alone (Supplemental Table S5, http://links.lww.com/HEP/J843) were independently associated with worse OS at 5 years.

Histologic subtypes can be identified by radiomics

CT scans were available for 50 subjects (Figures 6A, B); 21 (42%) were categorized as SBD type and 29 (58%) as LBD type. No differences in age and gender were observed in this subcohort compared to the entire cohort (Supplemental Table S6, http://links.lww.com/HEP/J843).

The WEKA Explorer Filter tool randomly subdivided the population into 2 groups: the first group, including 33 patients (66%), was used for model training, and the second group, made of 17 patients (34%), for model testing.

Two classifications were performed: SBD type versus LBD-type and PAS^{HIGH} LBD-type iCCA versus all other histotypes. Interestingly, radiomic features performed better than radiological morphological ones in discriminating SBD type from LBD-type and PAS^{HIGH} LBD-type iCCA from other histotypes (Supplemental Figure S10, http://links.lww.com/HEP/J845). The combination of radiomic and morphology features resulted in excellent accuracy in classifying cases as PAS^{HIGH} LBD-type iCCA and a very good accuracy in discriminating SBD type from LBD type, with AUCs of 0.942 and 0.847, respectively (Figure 6C). These observations were confirmed in a prospective validation cohort (Figure 6D and Supplemental Figure S10, http://links.lww.com/HEP/J845).

PAS^{HIGH} LBD-type iCCA is characterized by a cholestatic serological fingerprint

We explored differences in serum parameters of liver and biliary function among histological subtypes (Figure 7). There were no significant differences in

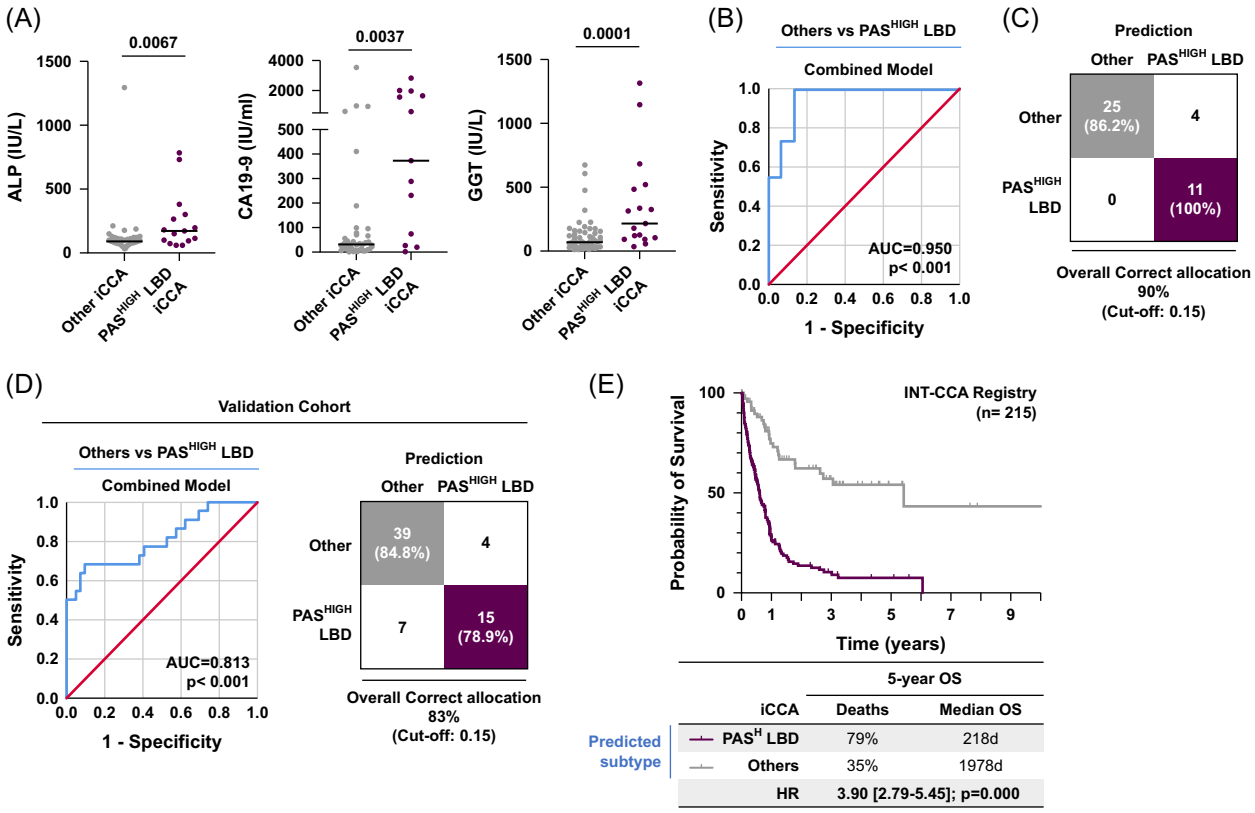

FIGURE 7 Serum signatures of intrahepatic cholangiocarcinoma (iCCA) subtypes. (A) Graphs report ALP, GGT, and CA19-9 serum levels in iCCA histological subtypes. Bars indicate mean values. Statistical significance was assessed by the Student *t* test. (B) ROC curve reports the accuracy of the combination of ALP, GGT, and CA19-9 (combined model) in discriminating PAS^{HIGH} LBD versus other iCCA histotypes. (C) Graph indicates the number (%) of cases correctly classified by the combined model as PAS^{HIGH} LBD versus other iCCA histotypes based on the best cutoff value for specificity and sensitivity (0.15). (D) Validation cohort: ROC curve reports accuracy of the combination of ALP, GGT, and CA19-9 (combined model) in discriminating PAS^{HIGH} LBD versus other iCCA histotypes; graph indicates the number (%) of cases correctly classified by the combined model as PAS^{HIGH} LBD versus other iCCA histotypes based on the best cutoff value (0.15). (E) Kaplan–Meier curve, aHR, and 95% CI for 5-year overall survival (OS) of patients from the INT-CCA clinical registry cohort based on predicted histological subtypes (PAS^{HIGH} LBD vs. other histotypes). Abbreviations: aHR, adjusted hazard ratio; CA19-9, carbohydrate antigen 19-9; iCCA, intrahepatic CCA; LBD, large bile duct type; PAS, Periodic acid of Schiff; ROC, receiver operating curve; SBD, small bile duct type.

ALT, AST, and CEA between LBD-type and SBD-type iCCAs (Supplemental Table S7, http://links.lww.com/HEP/J843); however, LBD showed higher values of ALP, GGT, and CA19-9 compared to SBD. Interestingly, PAS^{HIGH} LBD iCCA showed higher values of ALP, GGT, and CA19-9 but not ALT, AST, and CEA compared to other iCCA histotypes (Figure 7A). Therefore, we explored the potential role of ALP, GGT, and CA19-9 in discriminating PAS^{HIGH} LBD iCCA from other iCCA subtypes. The 3 tested biomarkers had a good accuracy in predicting the PAS^{HIGH} LBD iCCA type (Supplemental Figure S11, http://links.lww.com/HEP/J845), with an excellent accuracy (AUC = 0.950) when all 3 biomarkers were combined (Figure 7B).

These observations were confirmed in a prospective validation cohort (Figure 7D). Finally, based on the worst prognosis of PAS^{HIGH} LBD iCCA and the accuracy of a serum signature to identify this subtype, we retrieved a larger cohort (n = 215) of patients from the INT-CCA clinical registry to confirm the prognostic role of the serum fingerprint. Subjects affected by iCCA were divided based on the best cutoff value for specificity and sensitivity (Figure 7E); remarkably, subjects above the cutoff (putatively predictive for PAS^{HIGH} LBD histotype) showed a worse OS compared to those below the cutoff (Figure 7), after adjustment for age, gender, disease stage, and the presence of biliary disease or liver cirrhosis (Supplemental Table S8, http://links.lww.com/HEP/J843).

DISCUSSION

The main results obtained in the present study were: (i) the creation of a digitalized European CCA Histology Registry of tumors with associated clinical and radiological data, based on a multicenter and international European cohort; (ii) the definition of histological CCA subtypes with clinical and prognostic relevance; (iii) the use of radiomics and serum signatures for the classification of specific CCA histological subtypes.

International and multidisciplinary cooperation represents a key strategy for addressing rare cancers. To

facilitate this, ENSCCA has created interconnected registries (clinical, histological, radiological, molecular) as a strategic effort empowering CCA research. This approach is a prerequisite for the implementation of healthcare and research applications based on the digital twin paradigm.[21] Data obtained from the ENSCCA (INT-CCA) clinical registry (up to 2234 patients) provided the real-world landscape of CCA in Europe and provided diagnostic, prognostic, and therapeutic insights.[16]

Here, we report the creation of the European CCA Histology Registry. To date, it contains 293 CCA (main and validation cohorts) and nearly 1800 digital slides. Performed stains ensured an extensive characterization of tumor morphology, epithelial cell phenotype, and tissue microenvironment. The European CCA Histology Registry is an online platform potentially open for collegial revision of cases and teaching activities. Further, the availability of unstained sections ensures their usefulness for any future scientific collaborations and projects.

Histologically, CCAs are conventional adenocarcinomas. However, iCCA is highly variable, and different histological subtypes are well recognized. In the most recent World Health Organization classification, the 2 main histologic iCCA subtypes, the LBD type and SBD type, are documented based on the duct of origin and the tumor cell appearance.[18] The use of this classification was recently recommended in an EASL Clinical Practice Guideline as it offers insights into both the mutational landscape and prognosis.[5] Unfortunately, the adoption of variable criteria for the histological classification and the monocentric nature of literature studies limit the level of evidence and the strength of the recommendation.[9–12]

In general, the histologic subtyping of CCA can be challenging when only morphological criteria are used, especially in needle biopsies.[4] For example, the SBD type could invade larger ducts distally, or the LBD type can form nodular mass lesions as deeper stromal invasion occurs. In the present study, World Health Organization criteria were applied,[18] and tumors were histologically classified based on their morphology from H&E-stained sections. In our case series, equal numbers of iCCA were categorized as SBD or LBD type. Most pCCAs and all dCCAs were categorized as LBD, as expected based on the duct of origin (ie, hepatic ducts at hilum). Unexpectedly, a small number of pCCA cases (n = 2) were categorized as SBD type. This could be due to anatomical tumor misclassification, which can be challenging in some cases, especially in the locally advanced stage and in the presence of a mass-forming growth pattern.

High mucin content was frequently observed in p/dCCA and can be ascribed to the duct/cell of origin.[6] Mucin-containing and secreting cells are present in extrahepatic and large intrahepatic bile ducts, mainly in associated peribiliary glands.[22] According to the putative duct of origin, high mucin content was more frequently found in LBD-type iCCA compared to SBD-type iCCA. In LBD-type iCCA, PAS positivity could indicate a specific cell of origin with PAS^{HIGH} tumors resembling the phenotype of peribiliary glands and mucin-positive cells within the surface epithelium of larger intrahepatic bile ducts. This is in accordance with previous evidence indicating that peribiliary glands can show dysplastic features and undergo neoplastic transformation in human chronic biliary diseases[19] and in experimental models.[23,24] PAS^{HIGH} LBD iCCAs were associated with a high frequency of PNI in our cohort. This feature, also commonly observed in p/dCCA, could be ascribed to the growth pattern within the duct of origin; nerve branches within extrahepatic and large intrahepatic bile ducts could be rapidly infiltrated by the tumor cells growing with a periductal infiltrating pattern. Few SBD-type iCCA cases (n = 6) showed a PAS^{HIGH} phenotype and could be considered as an indeterminate/mixed pattern subtype (ie, mixtures of typical SBD with LBD-type areas or cuboidal tumor cells with abundant mucin production) as proposed recently.[25,26] This proposed approach is of value because, to date, there are no individual immunohistochemical markers that can discriminate with certainty between the SBD and LDB types. This point is particularly important in the diagnostic setting, when molecular studies should be prioritized when dealing with limited biopsy samples, as recommended by a recent consensus document.[27] Our approach, based on the combination of H&E-based morphological assessment and PAS stain, would potentially help in simplifying the histological subtyping, correlating clinical, radiological, and pathological features, and maximizing tissue usage for molecular-based patient management.

To further characterize the molecular features of tumor cells in the PAS^{HIGH} LBD-type iCCA, we performed spatial transcriptomic analysis and subsequently confirmed the most relevant differences in the entire cohort by immunohistochemistry. Interestingly, PAS^{HIGH} LBD showed higher EpCAM gene expression and immunohistochemical positivity compared to SBD iCCA. This is in line with the higher EpCAM expression found in healthy large bile ducts and associated peribiliary glands compared to interlobular bile ducts.[22] Contrastingly, SBD iCCAs were characterized by an upregulation in HIF1A and cyclin D1. In a previous study, impaired neoangiogenesis favoring lymphatic vessel formation was found in iCCA but not in pCCA.[28] In the whole cohort, we demonstrated a poorly vascularized stromal component in SBD-type iCCA by immunohistochemistry, which could explain the increased HIF1A expression. Although cyclin D1 was upregulated in SBD-type iCCA, no differences were found in MKI67 gene expression and in PCNA

protein expression by immunohistochemistry compared to PAS^{HIGH} LBD-type iCCA. Cyclin D1 expression can be induced by HIF1A;[29,30] therefore, we can speculate that this pathway is activated in the SBD type to support proliferation in a hypoxic environment.

From a methodological point of view, we demonstrated the usefulness of setting up a whole-slide imaging histological registry before moving to spatial-omics approaches. The European CCA Histology Registry allowed the selection of the most representative cases for molecular analysis based on a precise knowledge of the tissue architecture and patients' characteristics and served as the platform for confirming molecular results on a broader, well-characterized case series with complete clinical records.

From a clinical point of view, while no differences in 5-year OS were found between SBD-type and LBD-type iCCA, PAS^{HIGH} LBD iCCA represented the histologic subtype with the worst prognosis; high mucin content was associated with poor survival independently of SBD/LBD dichotomy, further strengthening the role of PAS positivity as a prognostic factor. Interestingly, PAS^{HIGH} LBD iCCA showed a serum fingerprint characterized by high values in ALP, GGT, and CA19-9, in contrast to other iCCA subtypes. The higher values in cholestatic indices could be due to an obstructive growth involving large intrahepatic bile ducts and/or concomitant cholangitis. Moreover, CA19-9 is a cell surface glycoprotein complex and is clinically associated with mucinous tumors.[31,32] Remarkably, these 3 serum biomarkers, alone or in combination, led to the accurate identification of PAS^{HIGH} LBD iCCA and were associated with a worse prognosis when tested on a larger case series.

The capability of radiomics and radiological morphological features in predicting iCCA histologic subtypes was also tested. Interestingly, a radiomic-based model was able to accurately identify PAS^{HIGH} LBD iCCA, suggesting the presence of specific radiologic textures detectable by imaging.[33]

Uniquely, an assessment of the surrounding liver and biliary tissues was performed in the present study. In Europe, iCCA is often considered to be a "sporadic" tumor and not associated with underlying liver disease except for primary sclerosing cholangitis.[1] However, nearly 2/3 of subjects affected by iCCA in our case series showed a significant histological liver parenchymal and/or biliary injury without differences between LBD versus SBD iCCA subtypes. Therefore, our observations seem to suggest that a pre-existing and clinically silent chronic liver/biliary condition (eg, steatotic liver disease, subclinical cholangitis) could be present in subjects who will develop iCCA. Further studies are essential to identify specific populations at risk and to develop appropriate screening protocols.

Limitations

The retrospective nature could be considered a limitation of the study; however, this allowed the collection of a cohort with a 5-year follow-up, and the inclusion of patients is still ongoing prospectively. Only subjects who underwent tumor resection were included, and we acknowledge that this subgroup of subjects may not fully represent CCA's natural history. However, resected tumor samples allowed a more accurate and in-depth histological analysis compared to needle biopsies and could give initial information to be evaluated in unresectable patients. The validation of our findings on independent cohorts would be needed to further translate them into clinics. Finally, the recruitment of subjects from additional European countries would enhance the geographic diversity of our cohort, thereby strengthening the conclusiveness of our results.

Perspectives and conclusions

Histological subtyping represents a cornerstone of prognosis and treatment in several cancers, including those of the breast and lung.[7,8] Our data indicate the importance of developing homogeneous morphological subclasses with a significant prevalence in CCA and allowing the potential role of histology as a cheap and easy means for risk stratification and prognosis. Future studies are important to address consensus on classification criteria and correlation with the complete molecular landscape of histological CCA subtypes. In conclusion, the European CCA Histology Registry represents a valuable resource and a platform for adopting an integrative approach to the study of CCA.

AUTHOR CONTRIBUTIONS

Concept and design: Guido Carpino, Diletta Overi, and Vincenzo Cardinale. Case/data acquisition: Vincenzo Cardinale, Pilar Acedo, Michail Doukas, Luca Di Tommaso, Pedro M. Rodrigues, Guido Torzilli, Manuela Martin-Izquierdo, Jose M. Hernández-Bayo, Laura Izquierdo-Sanchez, Diego Bueno-Sacristan, Ezio Lanza, Bas Groot Koerkamp, Andres Garcia-Sampedro, Stephen P. Pereira, Gian Luca Grazi, Domenico Alvaro, Jesus M. Banales, Ana Lleo, Rocio I.R. Macias, Felice Giuliante, Lara R. Heij, Julien Calderaro, Francesco Ardito, Konrad Reichel, Jérémy Augustin, Raffaele Brustia, Alberto Quaglia, Stefano Leone, Paolo Onori, Barbara Franceschini, Valeria Panebianco, Elio Damato, Agostino Maria De Rose, and Cristiana Soldani. Data analysis and interpretation: Guido Carpino, Diletta Overi, Vincenzo Cardinale, Timothy J. Kendall, Eugenio Gaudio, and Marco Rengo. Writing of the manuscript: Guido Carpino, Diletta Overi, and Marco Rengo. Critical revision of the manuscript for

important intellectual content: Vincenzo Cardinale, Pilar Acedo, Michail Doukas, Luca Di Tommaso, Pedro M. Rodrigues, Guido Torzilli, Manuela Martin-Izquierdo, Jose M. Hernández-Bayo, Laura Izquierdo-Sanchez, Diego Bueno-Sacristan, Ezio Lanza, Bas Groot Koerkamp, Andres Garcia-Sampedro, Stephen P. Pereira, Gian Luca Grazi, Domenico Alvaro, Jesus M. Banales, Ana Lleo, Rocio I.R. Macias, Felice Giuliante, Lara R. Heij, Julien Calderaro, Francesco Ardito, Konrad Reichel, Jérémy Augustin, Raffaele Brustia, Alberto Quaglia, Stefano Leone, Paolo Onori, Timothy J. Kendall, Barbara Franceschini, and Eugenio Gaudio. Final approval: Vincenzo Cardinale, Pilar Acedo, Michail Doukas, Luca Di Tommaso, Pedro M. Rodrigues, Guido Torzilli, Manuela Martin-Izquierdo, Jose M. Hernández-Bayo, Laura Izquierdo-Sanchez, Diego Bueno-Sacristan, Ezio Lanza, Bas Groot Koerkamp, Andres Garcia-Sampedro, Stephen P. Pereira, Gian Luca Grazi, Domenico Alvaro, Jesus M. Banales, Ana Lleo, Rocio I.R. Macias, Felice Giuliante, Lara R. Heij, Julien Calderaro, Francesco Ardito, Konrad Reichel, Jérémy Augustin, Raffaele Brustia, Alberto Quaglia, Stefano Leone, Paolo Onori, Barbara Franceschini, Timothy J. Kendall, Eugenio Gaudio, Marco Rengo, Diletta Overi, and Guido Carpino. Financial support: Eugenio Gaudio and Jesus M. Banales. Histology registry coordination: Guido Carpino, Diletta Overi, and Eugenio Gaudio. Radiology registry coordination: Marco Rengo, Rocio I.R. Macias, and Ana Lleo. Clinical registry coordination: Laura Izquierdo-Sanchez and Jesus M. Banales. Project supervisors: Ana Lleo, Rocio I.R. Macias, Jesus M. Banales, and Guido Carpino.

ACKNOWLEDGMENTS

None.

Presentation: preliminary data were presented at the Joint ENSCCA/Precision-BTC-Network Meeting in Krakow, Poland, July 1st–2nd, 2024.

FUNDING INFORMATION

This article is based upon work from the European Network for the Study of Cholangiocarcinoma and the COST Actions CA18122 European Cholangiocarcinoma Network (EURO-CHOLANGIO-NET) and CA22125 Precision Medicine in Biliary Tract Cancer (Precision-BTC-Network), supported by COST (European Cooperation in Science and Technology: www.cost.eu). Eugenio Gaudio, Diletta Overi, and Guido Carpino were funded by the European Union—Next Generation EU, Mission 4, Component 2, CUP B93D21010860004, Spoke 3, by Project PNC 0000001 D3 4 Health, CUP B53C22006120001, The National Plan for Complementary Investments to the NRRP, Funded by the European Union—NextGenerationEU, by PRIN 2022 (project no. 20222J7W2K), and by BIT-RD Biotecnology—Dulbecco Foundation (CUP: J53C23002920005). Vincenzo Cardinale and Domenico Alvaro were funded by Next Generation Europe Grant PE 6 FONDAZIONE HEAL ITALIA "Health Extended Alliance for Innovative Therapies, Advanced Lab-research and Integrated Approaches of Precision Medicine" PE_00000019—CUP B53C22004000006, and by Next Generation Europe Grant: Rome Technopole Flagship 4 (FP 4)—Development, innovation and certification of medical and non-medical devices for health (Decreto MUR del 23 giugno 2022 prot. no. 105; codice ECS 00000024). Domenico Alvaro, Vincenzo Cardinale, Guido Carpino, Eugenio Gaudio were funded by PRIN 2022 PNRR Funded by European Union - Next Generation EU (project n. P202222E45, CUP: B53D23031260001). Rocio I.R. Macias was supported by the Spanish Carlos III Health Institute (ISCIII) (FIS PI20/00189, PI23/00681). Stephen P. Pereira was supported by the National Institute for Health and Care Research, University College London Hospitals Biomedical Research Centre, UK. The research leading to these results has received funding from AIRC under IG 2020—ID. 25087 project—P.I.-Di Tommaso Luca. Ana Lleo received funding from the Associazione Italiana per la Ricerca sul Cancro (AIRC IG-2019-23408) and from the Italian Ministry of Health (NET-2019-12370049). Spanish Carlos III Health Institute (ISCIII) [Jesus M. Banales (FIS PI18/01075, PI21/00922 and Miguel Servet CPII19/00008); Pedro M. Rodrigues (FIS PI23/01850 and Miguel Servet CP22/00073); Jesus M. Banales (PMP21/00080)] cofinanced by "Fondo Europeo de Desarrollo Regional" (FEDER); CIBERehd (ISCIII): Jesus M. Banales, Pedro M. Rodrigues, and Laura Izquierdo-Sanchez, Spain; "Diputación Foral Gipuzkoa" (2023-CIEN-000008-01 to Pedro M. Rodrigues), Spain; Department of Health of the Basque Country (2020111077 and 2021111021 to Jesus M. Banales; 2022111070 to Pedro M. Rodrigues); La Caixa Scientific Foundation (Pedro M. Rodrigues: HR17-00601), Spain; "Fundación Científica de la Asociación Española Contra el Cáncer" (AECC Scientific Foundation: "Lab AECC 2023" AECC23/502 to Pedro M. Rodrigues; AECC Postdoctoral grant POST-D246369IZQU to Laura Izquierdo-Sanchez), Spain; Asociación Española para el Estudio del Hígado (AEEH, Juan Rodes Postdoctoral grant to Laura Izquierdo-Sanchez); AMMF—The Cholangiocarcinoma Charity (EU/2019/AMMFt/001 to Jesus M. Banales and Pedro M. Rodrigues), United Kingdom; PSC Partners US (to Jesus M. Banales) and PSC Supports UK (to Jesus M. Banales and Pedro M. Rodrigues). Laura Izquierdo-Sanchez received funds from the Department of Education of the Basque Country (POS_2022_1_0041).

CONFLICTS OF INTEREST

Vincenzo Cardinale received grants from Ipsen. Timothy J. Kendall consults for and is on the speakers' bureau for HistoIndex. He advises and is on the speakers' bureau for Jazz. He consults for Clinnovate

Health, Kynos, Perspectum, and Concept Life Sciences. He is on the speakers' bureau for AstraZeneca, Incyte, and Servier. He consults for or is on the speakers' bureau for Resolution. He is employed by Fibrofind. Ana Lleo consults for, is on the speakers' bureau for, and received grants from Ipsen. She consults for and is on the speakers' bureau for AlfaSigma, Advanz, GSK, and Gilead. She consults for and received grants from Dr. Falk. She consults for and is on the speakers' bureau for AstraZeneca. She consults for Albireo and Takeda. She is on the speakers' bureau for AbbVie, Incyte, Gore, and MSD. She received principal Investigator-associated institutional funding from Mirum, GSK, Ipsen, Dr. Falk, and Gilead. She received grants from the EU COST Action (CA22125), the Italian Ministry of Health, and the Italian Association for Cancer Research (AIRC). Jesus M. Banales consults for and received grants from Albireo and Cymabay. He is on the speakers' bureau and received grants from Incyte. He consults for Ikan Biotech, OWL-Rubió Metabolomics, Jazz, AstraZeneca, and Servier. He is on the speakers' bureau for AstraZeneca and Eisai, and Advanz. The remaining authors have no conflicts to report.

REFERENCES

1. Valle JW, Kelley RK, Nervi B, Oh DY, Zhu AX. Biliary tract cancer. Lancet. 2021;397:428–44.
2. Vogel A, Bridgewater J, Edeline J, Kelley RK, Klümpen HJ, Malka D, et al. Biliary tract cancer: ESMO Clinical Practice Guideline for diagnosis, treatment and follow-up. Ann Oncol. 2023;34:127–40.
3. Vithayathil M, Khan SA. Current epidemiology of cholangiocarcinoma in Western countries. J Hepatol. 2022;77:1690–8.
4. Kendall T, Verheij J, Gaudio E, Evert M, Guido M, Goeppert B, et al. Anatomical, histomorphological and molecular classification of cholangiocarcinoma. Liver Int. 2019;39(suppl 1):7–18.
5. European Association for the Study of the Liver. EASL–ILCA Clinical Practice Guidelines on the management of intrahepatic cholangiocarcinoma. J Hepatol. 2023;79:181–208.
6. Banales JM, Marin JJG, Lamarca A, Rodrigues PM, Khan SA, Roberts LR, et al. Cholangiocarcinoma 2020: The next horizon in mechanisms and management. Nat Rev Gastroenterol Hepatol. 2020;17:557–88.
7. Thai AA, Solomon BJ, Sequist LV, Gainor JF, Heist RS. Lung cancer. Lancet. 2021;398:535–54.
8. Loibl S, Poortmans P, Morrow M, Denkert C, Curigliano G. Breast cancer. Lancet. 2021;397:1750–69.
9. Akita M, Fujikura K, Ajiki T, Fukumoto T, Otani K, Azuma T, et al. Dichotomy in intrahepatic cholangiocarcinomas based on histologic similarities to hilar cholangiocarcinomas. Mod Pathol. 2017; 30:986–97.
10. Akita M, Sofue K, Fujikura K, Otani K, Itoh T, Ajiki T, et al. Histological and molecular characterization of intrahepatic bile duct cancers suggests an expanded definition of perihilar cholangiocarcinoma. HPB (Oxford). 2019;21:226–34.
11. Ma B, Meng H, Tian Y, Wang Y, Song T, Zhang T, et al. Distinct clinical and prognostic implication of IDH1/2 mutation and other most frequent mutations in large duct and small duct subtypes of intrahepatic cholangiocarcinoma. BMC Cancer. 2020;20:318.
12. Sigel CS, Drill E, Zhou Y, Basturk O, Askan G, Pak LM, et al. Intrahepatic cholangiocarcinomas have histologically and immunophenotypically distinct small and large duct patterns. Am J Surg Pathol. 2018;42:1334–45.
13. Fujii M, Sekine S, Sato T. Decoding the basis of histological variation in human cancer. Nat Rev Cancer. 2024;24:141–58.
14. Kather JN, Pearson AT, Halama N, Jäger D, Krause J, Loosen SH, et al. Deep learning can predict microsatellite instability directly from histology in gastrointestinal cancer. Nat Med. 2019; 25:1054–6.
15. Macias RIR, Cardinale V, Kendall TJ, Avila MA, Guido M, Coulouarn C, et al. Clinical relevance of biomarkers in cholangiocarcinoma: Critical revision and future directions. Gut. 2022;71:1669–83.
16. Izquierdo-Sanchez L, Lamarca A, La Casta A, Buettner S, Utpatel K, Klümpen HJ, et al. Cholangiocarcinoma landscape in Europe: Diagnostic, prognostic and therapeutic insights from the ENSCCA Registry. J Hepatol. 2022;76:1109–21.
17. Khan SA, Emadossadaty S, Ladep NG, Thomas HC, Elliott P, Taylor-Robinson SD, et al. Rising trends in cholangiocarcinoma: Is the ICD classification system misleading us? J Hepatol. 2012; 56:848–54.
18. Board WCoTE. Digestive System Tumours, Fifth Edition ed. Lyone (France): International Agency for Research on Cancer; 2019.
19. Carpino G, Cardinale V, Folseraas T, Overi D, Grzyb K, Costantini D, et al. Neoplastic transformation of the peribiliary stem cell niche in cholangiocarcinoma arisen in primary sclerosing cholangitis. Hepatology. 2019;69:622–38.
20. Brunt E, Aishima S, Clavien PA, Fowler K, Goodman Z, Gores G, et al. cHCC–CCA: Consensus terminology for primary liver carcinomas with both hepatocytic and cholangiocytic differentation. Hepatology. 2018;68:113–26.
21. Nagaraj D, Khandelwal P, Steyaert S, Gevaert O. Augmenting digital twins with federated learning in medicine. Lancet Digit Health. 2023;5:e251–3.
22. Carpino G, Cardinale V, Onori P, Franchitto A, Berloco PB, Rossi M, et al. Biliary tree stem/progenitor cells in glands of extrahepatic and intraheptic bile ducts: An anatomical in situ study yielding evidence of maturational lineages. J Anat. 2012; 220:186–99.
23. Hayata Y, Nakagawa H, Kurosaki S, Kawamura S, Matsushita Y, Hayakawa Y, et al. Axin2(+) peribiliary glands in the periampullary region generate biliary epithelial stem cells that give rise to ampullary carcinoma. Gastroenterology. 2021;160:2133–148.e6.
24. Nakagawa H, Suzuki N, Hirata Y, Hikiba Y, Hayakawa Y, Kinoshita H, et al. Biliary epithelial injury-induced regenerative response by IL-33 promotes cholangiocarcinogenesis from peribiliary glands. Proc Natl Acad Sci U S A. 2017;114:E3806–15.
25. Wang H, Chen J, Zhang X, Sheng X, Chang XY, Chen J, et al. Expert consensus on pathological diagnosis of intrahepatic cholangiocarcinoma (2022 version). J Clin Transl Hepatol. 2023;11:1553–64.
26. Komuta M. Intrahepatic cholangiocarcinoma: Histological diversity and the role of the pathologist. J Liver Cancer. 2024;24:17–22.
27. Kendall T, Overi D, Guido M, Braconi C, Banales J, Cardinale V, et al. Recommendations on maximising the clinical value of tissue in the management of patients with intrahepatic cholangiocarcinoma. JHEP Rep. 2024;6:101067.
28. Carpino G, Cardinale V, Di Giamberardino A, Overi D, Donsante S, Colasanti T, et al. Thrombospondin 1 and 2 along with PEDF inhibit angiogenesis and promote lymphangiogenesis in intrahepatic cholangiocarcinoma. J Hepatol. 2021;75:1377–86.
29. Mamo M, Ye IC, DiGiacomo JW, Park JY, Downs B, Gilkes DM. Hypoxia alters the response to anti-EGFR therapy by regulating EGFR expression and downstream signaling in a DNA methylation-specific and HIF-dependent manner. Cancer Res. 2020;80: 4998–5010.
30. Hubbi ME, Semenza GL. Regulation of cell proliferation by hypoxia-inducible factors. Am J Physiol Cell Physiol. 2015;309: C775–82.

31. Kamisawa T, Wood LD, Itoi T, Takaori K. Pancreatic cancer. Lancet. 2016;388:73–85.
32. Yousef A, Yousef M, Zeineddine MA, More A, Fanaeian M, Chowdhury S, et al. Serum tumor markers and outcomes in patients with appendiceal adenocarcinoma. JAMA Netw Open. 2024;7:e240260.
33. Granata V, Fusco R, Setola SV, Galdiero R, Maggialetti N, Patrone R, et al. Colorectal liver metastases patients prognostic assessment: Prospects and limits of radiomics and radio-genomics. Infect Agent Cancer. 2023;18:18.

How to cite this article: Carpino G, Overi D, Macias RI, Cardinale V, Izquierdo-Sanchez L, Acedo P, et al. Refinement of histologic subtypes and identification of biomarkers linked to unfavorable prognosis in cholangiocarcinoma: The ENSCCA registries' framework for digital twin advancement. Hepatology. 2026;83:753–770. https://doi.org/10.1097/HEP.0000000000001425